Hindawi Publishing Corporation
Journal of Chemistry
Volume 2014, Article ID 837682, 6 pages
http://dx.doi.org/10.1155/2014/837682

Research Article

One-Step Synthesis of Superparamagnetic Fe_3O_4@PANI Nanocomposites

Sanjeev Kumar and Sapna Jain

Department of Chemistry, University of Petroleum and Energy Studies, Dehradun 248007, India

Correspondence should be addressed to Sanjeev Kumar; sanjeevkumar.dubey2@gmail.com

Received 11 May 2013; Accepted 20 November 2013; Published 29 January 2014

Academic Editor: Theocharis C. Stamatatos

Monodisperse Fe_3O_4@PANI(Polyaniline) nanocomposites were successfully synthesized at ambient temperature via reverse microemulsion technique with the objective to gain control over the size and morphology of these nanocomposites. The present synthetic approach uses inexpansive $FeCl_3$ as a single iron source to prepare Fe_3O_4@PANI nanocomposites by the reverse microemulsion method. The obtained samples were characterized in detail by Fourier transform infrared spectroscopy, X-ray diffraction, transmission electron microscopy, and vibrating sample magnetometer. FTIR and X-ray diffractogram confirm the encapsulation of Fe_3O_4 nanoparticles by PANI. Highly monodisperse spherical Fe_3O_4@PANI nanocomposites with an average diameter of 60 nm have been produced. The-synthesized nanocomposites exhibit superparamagnetic behavior at room temperature under applied field. Also a novel mechanism employing $FeCl_3$ as a single iron source polymerizing aniline and simultaneously forming Fe_3O_4 is discussed.

1. Introduction

In recent years, interest has been focused on the design of the smart and intelligent multifunctional nanomaterials for technological applications and fundamental studies. To enable multifunctionality, several (multi)devices are stacked or combined and many different (multi)materials have to be used to achieve the desired functionality. Such multifunctional nanomaterials are often referred to as nanocomposites or core/shell nanoparticles, which include inorganic/inorganic hybrids and inorganic/organic hybrids. Fabrication involves the incorporation of the inorganic component and can provide a product with useful electrical, magnetic, or optical properties having wide range of applications [1–4]. In particular the nanomaterials in which both the phases are included are one of the most challenging targets of material science because it is not an easy task to characterize such complex nanoparticles from the viewpoint of the internal structures and the phase that gives rise to the internal structure and the phase that gives rise to magnetism. Today attention has been paid to synthesizing multifunctional nanocomposites with a magnetic core coated with conducting polymer via different synthetic routes such electrode deposition [5], in situ polymerization [6], electrochemical synthesis [7], and anodic oxidation [8]. However, only limited approaches have been used to develop a simple, mild, and efficient route to tune the properties of multicomponent ferrite/PANI(Polyaniline) nanocomposites [9]. Such nanocomposites have both high electrical and high magnetic permeability which required for the application in electrical and magnetic shielding, molecular electronics, nonlinear optics, biosensing, targeted drug delivery, and microwave absorbent [10–20]. Intrinsically conducting polymers are useful for a large number of applications: conducting paints and glues, solar cell, Schottky junctions, electromagnetic shielding autistatic formulations, sensors and actuators, electronic devices, and corrosion protection. Among all conducting polymers such as polypyrrole, polythiophene, and polyacetylene, polyaniline (PANI) has emerged as one of the most promising polymers because of its good environmental stability and controllable electrical properties [21]. Only in the intermediate oxidation state, the protonated emeraldine form is conducting and has been extensively studied for having interesting transport properties. This material is the alternating copolymer composed by the reduced and oxidized dimmer segments.

The great challenge for chemists is to design systems capable of spontaneously generating well-defined nanostructures by self-assembly from their components at a given set of conditions. On account that only limited approaches have been used to date, research is on to develop a simple, mild, and efficient route to control the architecture of final nanocomposites to fine-tune their properties [9, 22–26].

The present study is focused on synthesizing the polyaniline nanocomposites (Fe_3O_4@PANI nanocomposites) at ambient temperature via reverse microemulsion technique. Primary objective was to gain control over the size and morphology of these nanocomposites. To the best of our knowledge, the current synthetic approach is the first example using inexpensive $FeCl_3$ as single iron source to prepare Fe_3O_4/PANI nanocomposite by reverse microemulsion method.

2. Experimental Procedures

2.1. Materials. Anhydrous iron(III) chloride ($FeCl_3$, Sd Fine Chemicals, India), ammonium hydroxide solution (30 w%, SRL, India), cyclohexane (SRL, India), isoamyl alcohol (SRL, India), and Triton X-100 (SRL, India) were of analytical grade and used as received. Aniline monomer (SRL, India) was used after double distillation under reduced pressure and stored at low temperature (0–4°C).

2.1.1. Synthesis of the Magnetic Colloidal Solution. The magnetic colloidal solution containing Fe_3O_4 nanoparticles by reverse micelles process employing a quaternary system of cyclohexane/Triton X-100/isoamyl alcohol/H_2O was prepared. The two reverse micelles ME_1 and ME_2 were prepared. In a typical procedure, Triton X-100 was added to cyclohexane forming a murky emulsion. An aqueous solution of 0.5 M $FeCl_3{\cdot}6H_2O$ and isoamyl alcohol was then added to the emulsion under continuous magnetic stirring. The murky emulsion became transparent within seconds. The stirring was continued for 1 hour at room temperature resulting in a stable reverse micelle solution (ME_1). Reverse micelle solution (ME_2) was prepared under similar conditions by replacing $FeCl_3{\cdot}6H_2O$ with 30% solution of aq. ammonia.

The homogeneous reverse micelle solution ME_2 was then added dropwise to the reverse micelle solution ME_1 under constant magnetic stirring. Appearance of red brown colour after a few minutes marks the completion of the reaction and formation of magnetic colloidal solution. The pH of the reaction was maintained between 5 and 6. The whole reaction was carried out in an inert atmosphere. For characterization, the nanoparticles were separated by centrifugation followed by washing with methanol several times. The nanoparticles so-obtained were then dried in a vacuum oven at 100°C for 48 hours.

2.1.2. Synthesis of Fe_3O_4@PANI Nanocomposites. Reverse micelle solution ME_3 containing aniline monomer and 8 M HCl was prepared under identical conditions. The magnetic colloidal solution containing Fe_3O_4 nanoparticles was prepared by the same procedure as mentioned above. Now, this reverse micelle solution ME_3 was injected dropwise to a round bottom flask containing the fixed volume of magnetic colloidal solution containing Fe_3O_4 nanoparticles under continuous stirring. After 20–30 minutes, the color transforms from red brown to green confirming the polymerization of aniline. The reaction mixture was vigorously stirred for 24 hours using a mechanical stirrer. The whole reaction was carried out in an inert atmosphere at room temperature.

Acetone was added to precipitate Fe_3O_4/PANI nanocomposites and resulting precipitates were separated by subsequent centrifugation. The precipitates obtained were then washed several times with methanol and double-distilled water and then dried in a vacuum oven at 60°C for 72 hours.

2.2. Characterization. Fourier transform infrared (FTIR) spectroscopic measurements were taken on SHIMADZU Japan FTIR-8700 spectrophotometer. Samples of isolated particles of prepared nanoparticles were mixed with KBr, homogenized, and converted into pellets under a pressure of 8 tons and the spectra (% transmittance with wavenumber) were taken thereafter. The prepared nanoparticles were then characterized by the FTIR spectra.

The X-ray powder diffraction measurements were taken in a Philips PW 3040/60 X'Pert PRO (PANalytical) diffractometer (The Netherlands) using nickel-filtered Cu-Kα radiation at 1.54 Å. The resultant intensity data was processed using inbuilt PC-APD diffraction software to monitor the peak position and its corresponding intensity data correctly. The samples were placed on a slide and the measurements were taken continuously from 10° to 70° angles at 0.02° interval.

TEM measurements of the samples were taken on a Morgagni 268 D TEM, (The Netherlands) with a 70 kV accelerating voltage. The dispersions of nanoparticles in water were placed on carbon-coated 400 mesh copper grids and allowed to dry at room temperature before taking measurements. The obtained micrographs were then examined for particle shape and size.

Hysteresis loops of the powder samples were recorded in Lakeshore 7304 vibrating sample magnetometer (VSM).

3. Results and Discussions

3.1. Spectral Analysis. Typical FTIR spectra of bared Fe_3O_4, PANI and Fe_3O_4/PANI nanoparticles are shown in Figure 1. The FTIR spectra of PANI (Figure 1(b)) exhibit a peak at 3431 cm^{-1} attributed to N–H stretching vibration peak corresponding to PANI [27–29]. The peaks corresponding to benzenoid (NH–B–NH) and quinonoid (NH–Q–NH) rings are observed around 1590, 1500, and 1300 cm^{-1}, respectively [30, 31]. The peaks around 1160 cm^{-1} can be correlated with C=N stretching vibration [31]. The peak at 1160 cm^{-1}, corresponding to acid doping level, is smaller than typical PANI; therefore, our acid concentration is relatively low (high pH). FTIR spectra of bared Fe_3O_4 (Figure 1(a)) reveal the characteristic peak around 600 cm^{-1} and 440 cm^{-1} ascribed to the intrinsic vibration of the tetrahedral and octahedral sites, respectively [28, 29, 32].

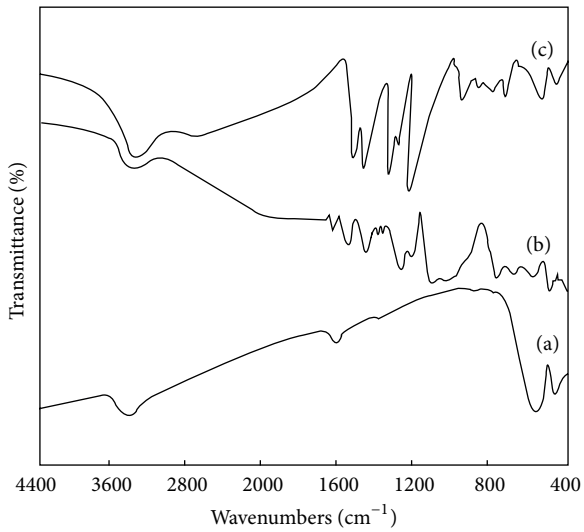

FIGURE 1: FTIR spectra of (a) Fe_3O_4 ferrite nanocrystals, (b) PANI, and (c) Fe_3O_4 ferrite/PANI nanocomposites.

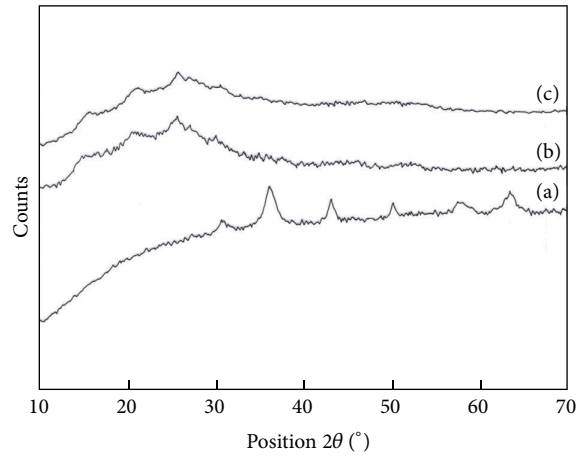

FIGURE 2: XRD patterns of (a) Fe_3O_4 ferrite nanocrystals, (b) PANI, and (c) Fe_3O_4/PANI nanocomposites obtained from reverse microemulsion.

Figure 1(c) shows the FTIR spectra of Fe_3O_4/PANI nanocomposite which are similar to the spectra of pure PANI. The characteristic peaks corresponding to Fe_3O_4 disappear in Fe_3O_4/PANI spectra indicating that the surface of the nanocomposite is composed of PANI. The peak around 1160 cm^{-1} intensifies in Fe_3O_4/PANI spectra showing the increased doping level (low pH) and thus confirming that pH plays an influential role in assigning the chain structure to PANI. The peak which arised between 700 and 590 cm^{-1} corresponds to C–Cl stretching confirming the Cl^- doping of polyaniline. In addition a peak appears around 1640 cm^{-1} which has been assigned to the carbonyl group (C=O), different from typical PANI, because of the quinone formation during polymerization [33]. The peaks of Fe_3O_4/PANI spectra shift towards lower wavenumber, probably due to the interaction of the 3d orbit of Fe_3O_4 with N atom in PANI to form a coordination bond. Thus, strong interaction of Fe_3O_4 nanoparticles with PANI backbone has been indicated by the FTIR spectra.

3.2. X-Ray Diffraction Analysis. X-ray diffraction has been used for structural determination of the-precipitated fine Fe_3O_4/PANI nanocomposite. Figure 2 shows the XRD pattern of bared Fe_3O_4 nanoparticles (Figure 2(a)) and Fe_3O_4/PANI nanocomposites (Figure 2(c)). Analysis of diffractogram (Figure 2(a)) reveals a strong reflection indexed to (311) plane which denotes the spinel phase and no characteristic peaks of impurities are detected, confirming the formation of the cubic spinel structure [34–36]. Figure 2(c) reveals a diffused broad amorphous halo over the 2-theta range of 6°–30° and three reflections around 15, 18, and 21° corresponding to large molecular weight polyaniline [37, 38]. This can be attributed to low crystallinity due to large fraction of PANI in nanocomposite [39]. Figure 2(b) shows that the characteristic peaks of Fe_3O_4 nanoparticles are broad and less intense, indicating the suppression of the crystalline behaviour of Fe_3O_4 which can be attributed to its encapsulation by PANI resulting in the constraint of Fe_3O_4 nanoparticles [25]. Also, planar configuration of polyaniline due to the densely packed phenyl rings and thus an extensive interchain Π-Π orbital overlap has been indicated by the presence of reflection around 2-theta value of 26° [40]. As suggested by FTIR spectra, investigation of X-ray diffractogram thus confirms the encapsulation of Fe_3O_4 nanoparticles by PANI. This observation is further corroborated by TEM studies.

3.3. Morphology. Transmission electron micrographs gave further insight into the structure of PANI-coated Fe_3O_4 nanoparticles. Typical TEM micrographs for the bared Fe_3O_4 and Fe_3O_4/PANI nanoparticles are shown in Figure 3. The TEM image of bared Fe_3O_4 nanoparticles shows that particles possess spherical morphology having a crystallite size of 3 nm (Figure 3(a)), whereas the TEM image of Fe_3O_4/PANI nanoparticles again shows the formation of spherical particles having an average diameter of 60 nm (Figure 3(b)). The dark region is Fe_3O_4 nanoparticles and the light colored region is PANI in Fe_3O_4/PANI nanocomposites. The TEM image of both the samples shows that nanoparticles are monodisperse in size as it is the main feature of this method.

4. Magnetic Properties

The room temperature hysteresis loop of all the samples was measured using vibrating sample magnetometer (VSM). Figure 4 shows their magnetization curves taken at room temperature (300 K). Typical sigmoidal shape of hysteresis loops has been observed, indicating a superparamagnetic property of the synthesized Fe_3O_4 ferrite nanocrystals (Figure 4(a)). It has been found that the hysteresis loop of Fe_3O_4 ferrite nanocrystals could not be saturated with the available maximum field. The hysteresis curve recorded at room temperature for Fe_3O_4 ferrite nanocrystals exhibits negligible coercivity and very low remanence, which would

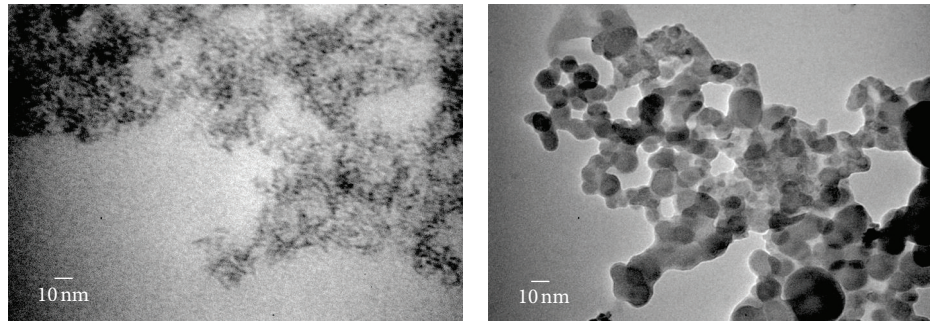

(a) (b)

Figure 3: (a) Magnetite nanoparticles and (b) Fe_3O_4/PANI nanocomposites.

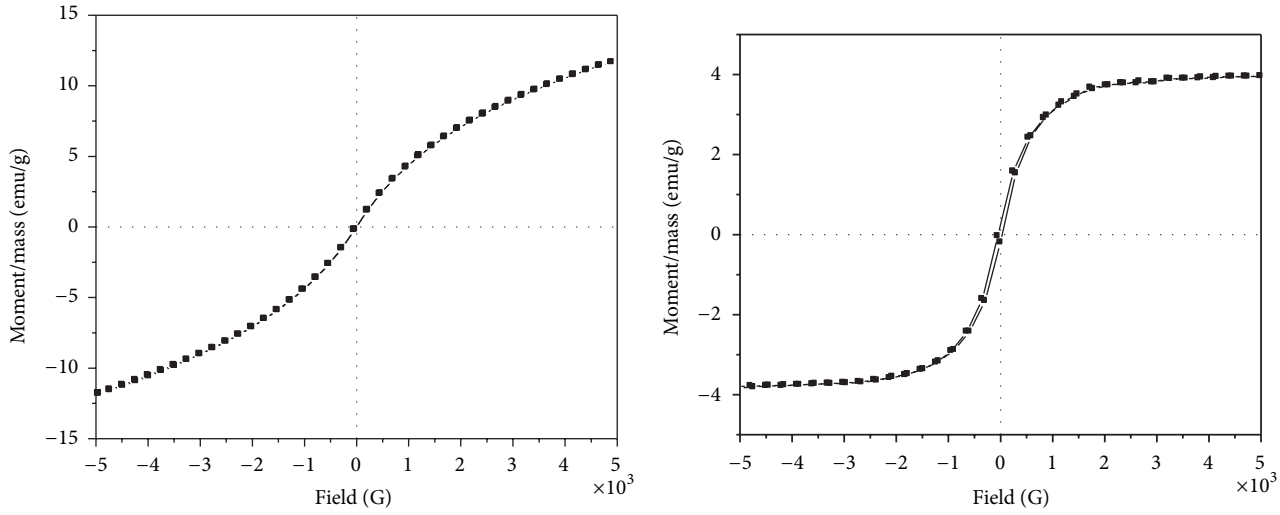

(a) (b)

Figure 4: The hysteresis loops of (a) Fe_3O_4 ferrite nanocrystals and (b) Fe_3O_4/PANI nanocomposites obtained from reverse microemulsion measured at 300 K.

be expected from these smaller size particles. This proves that the particles obtained from reverse microemulsion were superparamagnetic at room temperature [41, 42].

The magnetic hysteresis loop of Fe_3O_4 ferrite/PANI nanocomposite at room temperature is depicted in Figure 4(b). The magnetic properties were inherited from the magnetic Fe_3O_4 ferrite nanocrystals. The hysteresis loop for the nanocomposite gets saturated with the available maximum field indicating their ferromagnetic behavior. The saturation magnetization value of bimodal Fe_3O_4 ferrite/PANI nanocomposite was found to be 3.95 emu/g at 300 K with low coercive force (39 G). The interactions between the polymer and ferrite nanocrystals play a significant role in attaining the magnetic nature of these composites. The interaction between PANI nanofiber and Fe_3O_4 ferrite increases maybe due to H-bonding between –O– of ferrite and hydrogen of –N– of PANI nanofiber. Nanofiber has perfect geometrical orientation for strong H-bonding. Thus increased interactions between polymer and ferrite nanocrystals decrease the particle-particle exchange interaction due to which ferrite nanocrystals get aligned in applied magnetic field direction with PANI nanofiber effectively and Fe_3O_4 ferrite/PANI became ferromagnetic despite Fe_3O_4 ferrite being superparamagnetic.

4.1. Formation Mechanism of Nanocomposite. In accordance with the above results, a possible mechanism leading to Fe_3O_4/PANI nanocomposites has been proposed in (1). Ammonium hydroxide hydrolyses $FeCl_3$ to form ferric hydroxide ($Fe(OH)_3$). $Fe(OH)_3$ then takes up an electron from NH_2 group of aniline and generates a free radical and polymerizes aniline along with the generation of ferrous hydroxide ($Fe(OH)_2$). Ferrous hydroxide and ferric hydroxide react together to produce Fe_3O_4. As the reaction takes place in an inert atmosphere, oxygen (O_2) could not interfere with the reaction

$$\begin{aligned} FeCl_3 + 3NH_4OH &\longrightarrow Fe(OH)_3 + NH_4Cl \\ Fe(OH)_3 + \text{aniline} &\longrightarrow \text{Polyaniline} + Fe(OH)_2 \\ Fe(OH)_3 + Fe(OH)_2 &\longrightarrow Fe_3O_4 \longrightarrow Fe_3O_4/\text{PANI} \end{aligned} \quad (1)$$

5. Conclusion

In summary, a reverse microemulsion route has been reported, which is cost effective and promising to yield Fe_3O_4@PANI nanocomposites. In this versatile approach, highly monodisperse spherical nanocomposites with an average diameter of 60 nm have been produced. A novel mechanism employing $FeCl_3$ as a single iron source polymerizing aniline and simultaneously forming Fe_3O_4 is discussed. NH_2 group of aniline plays an important role in the formation of magnetite since it partly reduces Fe^{3+} to Fe^{2+} and also generates aniline free radical which undergoes free radical polymerization leading to PANI. This synthetic approach will pave the way for the preparation of monodisperse Fe_3O_4@PANI nanocomposites which would be extremely useful in a wide range of applications.

Conflict of Interests

The authors declare that there is no conflict of interests regarding the publication of this paper.

References

[1] J. G. Deng, C. L. He, Y. X. Peng et al., "Magnetic and conductive Fe_3O_4-polyaniline nanoparticles with core-shell structure," *Synthetic Metals*, vol. 139, no. 2, pp. 295–301, 2003.

[2] M. X. Wan and W. C. Li, "A composite of polyaniline with both conducting and ferromagnetic functions," *Journal of Polymer Science A*, vol. 35, no. 11, pp. 2129–2136, 1997.

[3] Z. Zhang and M. Wan, "Nanostructures of polyaniline composites containing nano-magnet," *Synthetic Metals*, vol. 132, no. 2, pp. 205–212, 2003.

[4] P. Gomez-Romero, "Hybrid organic-inorganic materials-in search of synergic activity," *Advanced Materials*, vol. 13, no. 3, pp. 163–174, 2001.

[5] D. Sazou, "Electrodeposition of ring-substituted polyanilines on Fe surfaces from aqueous oxalic acid solutions and corrosion protection of Fe," *Synthetic Metals*, vol. 118, no. 1–3, pp. 133–147, 2001.

[6] K. Sunderland, P. Brunetti, L. Spinu, J. Fang, Z. Wang, and W. Lu, "Synthesis of γ-Fe_2O_3/polypyrrole nanocomposite materials," *Materials Letters*, vol. 58, no. 25, pp. 3136–3140, 2004.

[7] O. Jarjayes, P. H. Fries, and C. Bidan, "New nanocomposites of polypyrrole including γ-Fe_2O_3 particles: electrical and magnetic characterizations," *Synthetic Metals*, vol. 69, no. 1–3, pp. 343–344, 1995.

[8] F. Yan, G. Xue, J. Chen, and Y. Lu, "Preparation of a conducting polymer/ferromagnet composite film by anodic-oxidation method," *Synthetic Metals*, vol. 123, no. 1, pp. 17–20, 2001.

[9] K. H. Wu, Y. M. Shin, C. C. Yang, W. D. Ho, and J. S. Hsu, "Preparation and ferromagnetic properties of $Ni_{0.5}Zn_{0.5}Fe_2O_4$/polyaniline core-shell nanocomposites," *Journal of Polymer Science A*, vol. 44, no. 8, pp. 2657–2664, 2006.

[10] Z. Wei, Z. Zhang, and M. Wan, "Formation mechanism of self-assembled polyaniline micro/nanotubes," *Langmuir*, vol. 18, no. 3, pp. 917–921, 2002.

[11] X. Sun, S. Dong, and E. Wang, "Large scale, templateless, surfactantless route to rapid synthesis of uniform poly(*o*-phenylenediamine) nanobelts ," *Chemical Communications*, no. 10, pp. 1182–1183, 2004.

[12] J. Huang and R. B. Kaner, "A general chemical route to polyaniline nanofibers," *Journal of the American Chemical Society*, vol. 126, no. 3, pp. 851–855, 2004.

[13] J. Huang and R. B. Kaner, "Nanofiber formation in the chemical polymerization of aniline: a mechanistic study," *Angewandte Chemie*, vol. 43, no. 43, pp. 5817–5821, 2004.

[14] C.-G. Wu and T. Bein, "Conducting polyaniline filaments in a mesoporous channel host," *Science*, vol. 264, no. 5166, pp. 1757–1759, 1994.

[15] J. Janata and M. Josowicz, "Conducting polymers in electronic chemical sensors," *Nature Materials*, vol. 2, no. 1, pp. 19–24, 2003.

[16] H. Naarmann, *Science and Application of Conducting Polymers*, Adam Hilger, Bristol, UK, 1991.

[17] A. P. Alivisatos, "Semiconductor clusters, nanocrystals, and quantum dots," *Science*, vol. 271, no. 5251, pp. 933–937, 1996.

[18] S. Sun, C. B. Murray, D. Weller, L. Folks, and A. Moser, "Monodisperse FePt nanoparticles and ferromagnetic FePt nanocrystal superlattices," *Science*, vol. 287, no. 5460, pp. 1989–1992, 2000.

[19] F. X. Redl, K.-S. Cho, C. B. Murray, and S. O'Brien, "Three-dimensional binary superlattices of magnetic nanocrystals and semiconductor quantum dots," *Nature*, vol. 423, no. 6943, pp. 968–971, 2003.

[20] J. Park, J. Joo, G. K. Soon, Y. Jang, and T. Hyeon, "Synthesis of monodisperse spherical nanocrystals," *Angewandte Chemie*, vol. 46, no. 25, pp. 4630–4660, 2007.

[21] D. C. Trivedi, *Handbook of Organic Conductive Molecule and Polymers*, vol. 2, John Wiley & Sons, Chichester, UK, 1997.

[22] G. Xie, Q. Zhang, Z. Luo, and M. Wu T, "Preparation and characterization of monodisperse magnetic poly(styrene butyl acrylate methacrylic acid) microspheres in the presence of a polar solvent," *Journal of Applied Polymer Science*, vol. 87, no. 11, pp. 1733–1738, 2003.

[23] J. Alam, U. Riaz, and S. Ahmad, "Effect of ferrofluid concentration on electrical and magnetic properties of the Fe_3O_4/PANI nanocomposites," *Journal of Magnetism and Magnetic Materials*, vol. 314, no. 2, pp. 93–99, 2007.

[24] L. Bao and J. S. Jiang, "Evolution of microstructure and phase of Fe_3O_4 in system of Fe_3O_4-polyaniline during high-energy ball milling," *Physica B*, vol. 367, no. 1–4, pp. 182–187, 2005.

[25] S. Xuan, Y.-X. J. Wang, K. C.-F. Leung, and K. Shu, "Synthesis of Fe_3O_4@polyaniline core/shell microspheres with well-defined blackberry-like morphology," *Journal of Physical Chemistry C*, vol. 112, no. 48, pp. 18804–18809, 2008.

[26] H. Zhong-ai, Z. Hong-Xiao, K. Chao et al., "The preparation and characterization of quadrate $NiFe_2O_4$/polyaniline nanocomposites," *Journal of Materials Science: Materials in Electronics*, vol. 17, no. 11, pp. 859–863, 2006.

[27] P. Dallas, D. Stamopoulos, N. Boukos, V. Tzitzios, D. Niarchos, and D. Petridis, "Characterization, magnetic and transport properties of polyaniline synthesized through interfacial polymerization," *Polymer*, vol. 48, no. 11, pp. 3162–3169, 2007.

[28] L. A. Garcia-Cerda and S. M. Montemayor, "Synthesis of $CoFe_2O_4$ nanoparticles embedded in a silica matrix by the citrate precursor technique," *Journal of Magnetism and Magnetic Materials*, vol. 294, no. 2, pp. e43–e46, 2005.

[29] Y. Ahn, E. J. Choi, and E. H. Kim, "Superparamagnetic relaxation in cobalt ferrite nanoparticles sysnthesized from hydroxide carbonate precursors," *Reviews on Advanced Materials Science*, vol. 5, no. 5, pp. 477–480, 2003.

[30] J. Stejskal, I. Sapurina, M. Trchová, E. N. Konyushenko, and P. Holler, "The genesis of polyaniline nanotubes," *Polymer*, vol. 47, no. 25, pp. 8253–8262, 2006.

[31] E. N. Konyushenko, J. Stejskal, I. Šeděnková et al., "Polyaniline nanotubes: conditions of formation," *Polymer International*, vol. 55, no. 1, pp. 31–39, 2006.

[32] N. Wu, L. Fu, M. Su, M. Aslam, K. C. Wong, and V. P. Dravid, "Interaction of fatty acid monolayers with cobalt nanoparticles," *Nano Letters*, vol. 4, no. 2, pp. 383–386, 2004.

[33] K. Landfester, "Miniemulsions for nanoparticle synthesis," in *Colloid Chemistry II*, vol. 227, pp. 75–123, Springer, Berlin, Germany, 2003.

[34] G. Vaidyanathan, S. Sendhilnathan, and R. Arulmurgan, "Structural and magnetic properties of $Co_{1-x}Zn_xFe_2O_4$ nanoparticles by co-precipitation method," *Journal of Magnetism and Magnetic Materials*, vol. 313, no. 2, pp. 293–299, 2007.

[35] C. Caizer and M. Stefanescu, "Magnetic characterization of nanocrystalline Ni-Zn ferrite powder prepared by the glyoxylate precursor method," *Journal of Physics D*, vol. 35, no. 23, pp. 3035–3040, 2002.

[36] C. Dong, "PowderX: windows-95-based program for powder X-ray diffraction data processing," *Journal of Applied Crystallography*, vol. 32, part 4, p. 838, 1999.

[37] H. Gao, T. Jiang, B. Han et al., "Aqueous/ionic liquid interfacial polymerization for preparing polyaniline nanoparticles," *Polymer*, vol. 45, no. 9, pp. 3017–3019, 2004.

[38] J. P. Pouget, M. E. Józefowicz, A. J. Epstein, X. Tang, and A. G. MacDiarmid, "X-ray structure of polyaniline," *Macromolecules*, vol. 24, no. 3, pp. 779–789, 1991.

[39] Ö. Yavuz, M. K. Ram, M. Aldissi, P. Poddar, and S. Hariharan, "Synthesis and the physical properties of MnZn ferrite and NiMnZn ferrite-polyaniline nanocomposite particles," *Journal of Materials Chemistry*, vol. 15, no. 7, pp. 810–817, 2005.

[40] W. Luzny, M. Sniechowski, and J. Laskab, "Structural properties of emeraldine base and the role of water contents: X-ray diffraction and computer modelling study ," *Synthetic Metals*, vol. 126, no. 1, pp. 27–35, 2002.

[41] T. Upadhayay, R. V. Upadhayay, and R. V. Mehta, "Characterization of a temperature-sensitive magnetic fluid," *Physical Review B*, vol. 55, no. 9, pp. 5585–5588, 1997.

[42] S. Xaun, L. Hao, W. Jiang, X. Gong, Y. Hu, and Z. Chen, "Preparation of water-soluble magnetite nanocrystals through hydrothermal approach," *Journal of Magnetism and Magnetic Materials*, vol. 308, no. 2, pp. 210–213, 2007.